

Constraints on leptophilic dark matter from the AMS-02 experiment

L. Ali Cavasonza ^{*1}, H. Gast ¹, M. Krämer ², M. Pellen ³, and S. Schael ¹

¹*I. Physikalisches Institut, RWTH Aachen University, Sommerfeldstr. 14, 52074 Aachen, Germany*

²*Institute for Theoretical Particle Physics and Cosmology, RWTH Aachen University, 52074 Aachen, Germany*

³*Universität Würzburg, Institut für Theoretische Physik und Astrophysik, D-97074 Würzburg, Germany*

May 10, 2017

Abstract

The annihilation of dark matter particles in the Galactic halo of the Milky Way may lead to cosmic ray signatures that can be probed by the AMS-02 experiment, which has measured the composition and fluxes of charged cosmic rays with unprecedented precision. Given the absence of characteristic spectral features in the electron and positron fluxes measured by AMS-02, we derive upper limits on the dark matter annihilation cross section for leptophilic dark matter models. Our limits are based on a new background model that describes all recent measurements of the energy spectra of cosmic-ray positrons and electrons. For thermal dark matter relics, we can exclude dark matter masses below about 100 GeV. We include the radiation of electroweak gauge bosons in the dark matter annihilation process and compute the antiproton signal that can be expected within leptophilic dark matter models.

*E-mail: cavasonza@physik.rwth-aachen.de

1 Introduction

The AMS-02 Collaboration has published the most precise, separate measurements of the fluxes Φ_{\pm} of cosmic-ray electrons and positrons to date [1]. The data cover particle energies E up to 500 GeV for positrons and 700 GeV for electrons, respectively. These measurements are inconsistent with pure secondary production. This observation is among the most intriguing in cosmic ray physics, and various models have been proposed in the literature to explain the AMS-02 data. Most models invoke either exotic new physics like annihilations of dark matter particles, *e.g.* [2–4], or new astrophysical sources like pulsars and their wind nebulae, *e.g.* [3, 5, 6], to explain the apparent excess of positrons.

Advocating a pure dark matter origin for the large amount of positrons observed in cosmic rays at high energies would require a rather contrived scenario [3, 7–14], as very large cross sections are necessary to accommodate the measured fluxes. For this reason hybrid models are introduced in which an unspecified astrophysical background creates a smooth spectrum of positrons (and electrons), while dark matter could be responsible for small additional spectral features on top of the smooth background curve, *e.g.* [15, 16]. Previous studies *e.g.* [15] employed the positron fraction ($e^{+}/(e^{+}+e^{-})$) data from AMS and the simplified phenomenological model introduced by the AMS Collaboration [17]. The overall normalisation of the electron flux, needed to compare model predictions to data, was then often derived from the measurement of the $e^{+}+e^{-}$ flux by the Fermi-LAT detector. This approach, however, is problematic for several reasons: First, meanwhile the AMS $e^{+}+e^{-}$ data have been published. While the AMS data sets are self-consistent, *i.e.* one can derive both the positron fraction and the $e^{+}+e^{-}$ flux from the individual fluxes and conversely, the AMS $e^{+}+e^{-}$ flux is not consistent with the Fermi-LAT $e^{+}+e^{-}$ flux within the quoted experimental uncertainties. Therefore these two data sets cannot be combined in a fit in a trivial way. Second, the uncertainties on the energy scales have to be taken into account when combining data sets from different experiments. Third, the data from AMS and from Fermi-LAT were taken at different times. The model introduced in [17] to describe the positron fraction does not contain any time dependent parameters. The data from previous experiments and the data from AMS [18] clearly show a time variation of the positron fraction at energies below ~ 20 GeV. To avoid these issues we use only the published data from AMS and we introduce a new phenomenological model that properly describes the energy and time dependence of both cosmic-ray positrons and electrons. We determine the best-fit values of the model parameters, and discuss how the model can be applied for searches of spectral signatures of exotic processes using the AMS data. We consider a generic leptophilic dark matter model and derive upper limits on the dark matter annihilation cross section from the absence of characteristic spectral features in the electron and positron fluxes measured by AMS-02. We also assess the impact of the uncertainty from cosmic ray propagation and the dark matter halo model on the cross section limits. Electroweak gauge boson radiation in the dark matter annihilation process will lead to a flux of Standard Model particles from the decay and hadronisation of the electroweak gauge bosons, including in particular antiprotons. We show that the antiproton flux provides a sensitive and complementary probe of dark matter models, even within the leptophilic scenario we consider.

The article is structured as follows: In section 2 we discuss the class of dark matter models we consider and describe how we obtain the electron and positron fluxes due to dark matter annihilation in the Galactic halo. The new background model is introduced in section 3 where we also determine the best-fit values of the model parameters. The calculation of the limits on the dark matter annihilation cross section from AMS-02 data is presented in section 4. Antiproton fluxes are generated from the radiation of electroweak gauge bosons and may lead to complementary constraints on the dark matter model, as discussed in section 5. We summarise and conclude in section 6.

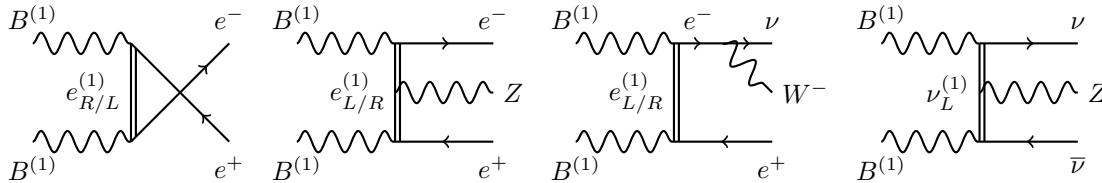


Figure 1: Contributions to Kaluza-Klein photon annihilation into an electron-positron/neutrino-antineutrino pair, including electroweak radiation.

2 Dark matter searches

A large number of possible extensions of the Standard Model providing viable dark matter candidates has been proposed. In our analysis we consider leptophilic dark matter, and specifically scenarios where dark matter couples at lowest order only to electron-positron pairs. In fact, within leptophilic models one has the highest sensitivity when comparing to the AMS measurements of electron and positron fluxes. Moreover, the role of electroweak radiation in these models is particularly significant, as fluxes of all stable Standard Model particles are induced, even though the dark matter couples directly only to charged leptons. Given the absence of distinctive spectral features in the AMS-02 positron and electron fluxes, we obtain constraints on this class of dark matter models.

At leading order, the upper limits on the dark matter annihilation cross section we derive do not depend on the specific choice of the model, but apply to leptophilic models in general. For the inclusion of electroweak radiation, however, one needs to consider a specific model, as the model-independent fragmentation function approach [19] can only be used for dark matter masses much larger than those of the electroweak gauge bosons, $M_{\text{DM}} \gg M_{W/Z}$ [20].

To calculate the electroweak radiation we thus consider a simple model with a t/u -channel fermionic mediator and a vector dark matter candidate, as predicted in theories with Universal Extra Dimensions (UED) [21, 22]. In such UED type models, the first Kaluza-Klein excitation of the $U(1)_Y$ hypercharge gauge field, $B^{(1)}$, provides the dark matter candidate. At leading order, the annihilation process is: $B^{(1)}B^{(1)} \rightarrow e^+e^-/\bar{\nu}\nu$. It is mediated by t - and u -channel exchange of the first Kaluza-Klein excitation of the electron, $e_{L,R}^{(1)}$ and of the neutrino $\nu_L^{(1)}$. The electron and positron fluxes are obtained considering the primary fluxes from dark matter annihilation (in this case the energy spectrum is simply a delta function at $E = M_{\text{DM}}$), taking into account the particle physics evolution of the primary decay products and propagating the particles through the Galaxy. This model is not helicity suppressed like supersymmetric scenarios with Majorana dark matter and thus the induced electron and positron fluxes lead to sharp features on top of the astrophysical fluxes. In addition, we study the effect of electroweak radiation in the calculation of the annihilation cross section and in the generation of the fluxes. To this end, we consider the processes $\text{DM} + \text{DM} \rightarrow e^+ + e^-$, $\text{DM} + \text{DM} \rightarrow e^+ + e^- + Z$, $\text{DM} + \text{DM} \rightarrow e^- + \bar{\nu} + W^+$, $\text{DM} + \text{DM} \rightarrow e^+ + \nu + W^-$ and $\text{DM} + \text{DM} \rightarrow \nu + \bar{\nu} + Z$.¹ Representative Feynman diagrams for each channel are shown in Fig. 1. To obtain the signal from dark matter annihilation at Earth we first generate the hard process, using an in-house Monte Carlo program. The matrix elements have been obtained with CalcHep [23, 24] and have been checked against MadGraph_aMC@NLO [25]. The evolution of the primary annihilation products (QED and QCD radiation, decays and hadronisation) has been taken into account using PYTHIA 8 [26].

For the description of the propagation of cosmic ray particles, a Green function formalism [27] has been used. The Navarro-Frenk-White (NFW) [28, 29] model for the dark matter profile and

¹For the study of positrons and antiprotons fluxes, the channel $\text{DM} + \text{DM} \rightarrow \nu + \bar{\nu}$ is irrelevant, nonetheless it is necessary to preserve gauge invariance when including electroweak corrections.

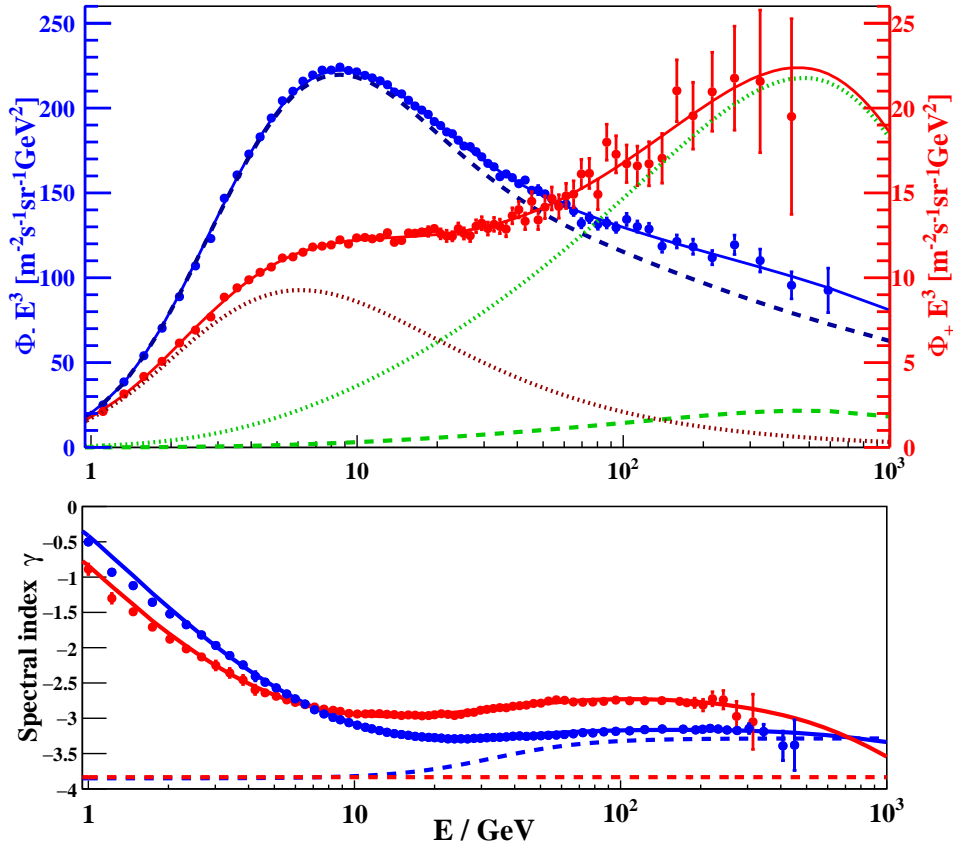


Figure 2: Top panel: electron (blue circles) and positron (red circles) fluxes measured by AMS and multiplied by E^3 , as described in the text. The best fit model curve (blue solid line for positrons and red solid line for electrons) according to Eqs. (2) are shown for energies above $E \geq 1$ GeV. The separate contributions from the diffuse (dotted red and dashed blue for positrons and electrons, respectively) and source term (dotted green and dashed green for positrons and electrons, respectively) are also shown. Bottom panel: spectral index $d \log \Phi / d \log E$ obtained from sliding-window fits to data. The solid line represents the spectral index obtained from the fit. The red and blue dashed lines represent the diffuse component for positrons and electrons, respectively, and clearly show the different behaviour of electrons and positrons.

the MED astrophysics scenario described in [27, 30] has been used. The value for the dark matter density at the location of the Sun has been taken to be $\rho = 0.3 \text{ GeV}/\text{cm}^3$ [31].

3 Background model

An accurate modelling of the fluxes of astrophysical origin is crucial for dark matter searches. A successful description from first principles of the available measurements of electrons, positrons, protons, antiprotons and nuclei, has not been proposed yet. On the other hand, considering only the electron and positron data, a description in terms of secondary production and astrophysical sources is possible, as done for instance in [32]. In the following, we search for sharp spectral features due to leading-order dark matter annihilation into electron-positron pairs on top of such an astrophysical background that is assumed to be smooth. For this reason, a simple phenomenological description of the background fluxes is suitable for our study.

For the description of their data on the positron fraction, the AMS Collaboration introduced

the so-called minimal phenomenological model [17]:

$$\Phi_+(E) = C_+ E^{-\gamma_+} + C_S E^{-\gamma_S} \exp(-E/E_S), \quad (1a)$$

$$\Phi_-(E) = C_- E^{-\gamma_-} + C_S E^{-\gamma_S} \exp(-E/E_S), \quad (1b)$$

and found that it describes their data extremely well over the full energy range. In fact, the minimal model works also for the description of the positron flux measured by AMS, provided that the effects of solar modulation are described in terms of the so-called force-field approximation [33]. However, trying to fit the electron flux with the same approach leads to a very poor fit with a $\chi^2/d.o.f. \sim 340/65$. Therefore, we introduce a generalised, phenomenological model that contains a smoothly-broken power law for the electrons, to describe the two components expected in the electron flux, namely secondary production and primary electrons from astrophysical sources:

$$\Phi_+(E) = (E^2/\hat{E}^2)(C_+(\hat{E}/E_0)^{-\gamma_+} + C_S(\hat{E}/E_1)^{-\gamma_S} \exp(-\lambda_S \hat{E})), \quad (2a)$$

$$\Phi_-(E) = (E^2/\hat{E}^2)(C_-(\hat{E}/E_0)^{-\gamma_-}(1 + (\hat{E}/E_B)^{\frac{1}{b}})^{b\Delta\gamma_-} + C_S(\hat{E}/E_1)^{-\gamma_S} \exp(-\lambda_S \hat{E})). \quad (2b)$$

This model contains the minimal number of parameters necessary to obtain an accurate description of both electron and positron fluxes. Here, $\hat{E} = E + \varphi_{\pm}$ is the energy of particles in interstellar space, before interacting with the heliosphere, and the effective potentials φ_{\pm} account for the charge-sign dependent impact of the solar magnetic field. In this picture, the solar modulation potentials are the only parameters that are expected to exhibit a time dependence.

The spectral indices for the diffuse terms of positrons and electrons and the common source term are denoted by γ_+ , γ_- and γ_S , respectively, E_B is the location of the spectral break and $\Delta\gamma_-$ is the difference of the electrons' spectral indices before and after the break. The smoothness of the break is described by the parameter b . The inverse cutoff energy is given by λ_S , and the C_{\pm} and C_S denote flux amplitudes. With this phenomenological model, we are able to describe electron and positron fluxes above 1 GeV.

We have explicitly included the pivot energies E_0 and E_1 in the model. They are fixed numbers that can, in principle, be chosen at will. However, a proper choice will substantially reduce the correlations between the model parameters in the fit used to extract the parameters of the model and increase the stability of the fit. We will use $E_0 = 5$ GeV and $E_1 = 60$ GeV throughout. We will refer to the first term in the fluxes as the *diffuse* term and to the second term as the *source* term, but this need not be related to the actual physics behind the fluxes. In this model the source term is assumed to be charge symmetric, since no evidence for a deficit of electrons has been observed so far. This hypothesis can be tested with the current AMS measurements of lepton fluxes.

To determine the parameters of the model, we perform a χ^2 minimisation using the AMS data on the separate measurements of cosmic ray electron and positron fluxes [1]. We also include the last data point of the AMS measurement of the total $e^+ + e^-$ flux [34], covering the energy range from 700 to 1000 GeV, since it is statistically independent from the other data and contains additional information for the modelling at the highest energies. The χ^2 is obtained by adding the contributions from these three different data sets.

The systematic uncertainties quoted by the AMS Collaboration vary as a function of energy in the range between 3% – 17%. Using these systematic uncertainties the $\chi^2/n.d.f.$ of the fit is significantly smaller than one, showing that the systematic uncertainties are correlated between energy bins, as expected from the description of the sources of the systematic uncertainties in the corresponding publications. A correct treatment of these correlations would require the knowledge of the correlation matrix, which is not published. In this case, the simplest assumption is that the systematic uncertainties consist of an uncorrelated component and a 100% correlated component. Therefore, for each data point, we take the published statistical uncertainty into

account, and we add an uncorrelated systematic uncertainty of only 1% in quadrature. We treat the remaining uncertainty with respect to the published one as an overall scale uncertainty on the acceptance, which effectively translates into an uncertainty on the normalisation of the fluxes. A similar procedure was used by the AMS Collaboration in [35]. With this prescription we find a $\chi^2/n.d.f. \sim 1$ and an unbiased pull-distribution. The fit of the positron flux alone would not allow us to constrain the model parameters of the source term with sufficient accuracy to derive limits on a possible dark matter contribution.

The best-fit parameters and their uncertainties σ_{fit} are listed in Table 1. The $\chi^2/n.d.f.$ is 131/128. The corresponding model curves are illustrated in Fig. 2 for both electrons and positrons. The same set of parameters gives good descriptions of the positron fraction and of the $e^+ + e^-$ flux measured by AMS.

parameter	value		σ_{fit}		σ_{acc}		σ_{scale}	
C_-	6.673	\pm	0.183	\pm	0.013	\pm	1.052	$\text{GeV}^{-1} \text{m}^{-2} \text{sr}^{-1} \text{s}^{-1}$
γ_-	3.851	\pm	0.031	\pm	0.007	\pm	0.087	
$\Delta\gamma_-$	5.650	\pm	0.561	\pm	0.105	\pm	0.881	$\times 10^{-1}$
b	4.171	\pm	0.675	\pm	0.078	\pm	0.466	$\times 10^{-1}$
$1/E_b$	3.043	\pm	0.189	\pm	0.045	\pm	0.250	$\times 10^{-2} \text{GeV}^{-1}$
C_+	2.161	\pm	0.065	\pm	0.014	\pm	0.305	$\times 10^{-1} \text{GeV}^{-1} \text{m}^{-2} \text{sr}^{-1} \text{s}^{-1}$
γ_+	3.834	\pm	0.107	\pm	0.007	\pm	0.106	
C_S	6.189	\pm	0.322	\pm	0.058	\pm	0.494	$\times 10^{-5} \text{GeV}^{-1} \text{m}^{-2} \text{sr}^{-1} \text{s}^{-1}$
γ_S	2.525	\pm	0.120	\pm	0.006	\pm	0.045	
λ_S	1.019	\pm	0.727	\pm	0.251	\pm	0.141	$\times 10^{-3} \text{GeV}^{-1}$
φ_-	1.406	\pm	0.023	\pm	0.027	\pm	0.096	GV
φ_+	1.021	\pm	0.048	\pm	0.022	\pm	0.082	GV

Table 1: Best-fit parameters for the model defined by Eqs. (2), with parameter uncertainties due to statistical and uncorrelated systematic uncertainties of the data (σ_{fit}), correlated systematic uncertainties (σ_{acc}), and energy scale uncertainties (σ_{scale}).

To evaluate the scale uncertainty σ_{acc} introduced by the correlated systematic uncertainties on the fit parameters, we use the shift method [36]: We subtract the 1% error from the quoted systematic uncertainties in quadrature, shift the data points upward by the remaining amount, and repeat the fit. The same procedure is repeated for shifting the data points downward. The value of σ_{acc} is then taken as the average observed shift in the parameters from the two fits. The resulting uncertainties (*cf.* Table 1) are small compared to the respective values of σ_{fit} , except for those of the solar modulation parameters φ_+ and φ_- , for which they are of equal magnitude. We also investigate the effect of the overall uncertainty of the energy scale of the AMS detector on the fit results. The AMS Collaboration quotes uncertainties of 5% at 0.5 GeV, 2% in the range from 10 to 290 GeV, and 4% at 700 GeV [1], and we connect these values by straight lines in $\log(E)$. The impact of the energy scale uncertainty on the fit parameters can then be studied by changing the energy bin boundaries of the data by the appropriate amount and correcting the integral flux values accordingly. The procedure is done for the two most extreme cases, shifting all energies upward and downward, respectively. The corresponding uncertainty σ_{scale} is calculated as the average of the observed shifts in the parameters. It turns out that this uncertainty is sizeable or even dominant for almost all of the fit parameters.

Finally, we tested if our model can also be used to describe the measurements of the positron flux by Pamela [37] and of the electron flux by Pamela [38] and Fermi-LAT [39]. We fix all parameters except C_+ and C_- . This accounts for a possible difference in the energy scale between the experiments, which would in the simplest case translate to a difference in the normalisations of the fluxes. In addition, since the data sets were recorded at different times,

we allow the modulation parameters φ_{\pm} to vary. We find in each case a $\chi^2/n.d.f. < 1$ and the best-fit values $C_+ = (1.76 \pm 0.12) \times 10^{-1} \text{ GeV}^{-1} \text{ m}^{-2} \text{ sr}^{-1} \text{ s}^{-1}$ and $\varphi_+ = (0.67 \pm 0.04) \text{ GV}$ for the Pamela positron flux, $C_- = (5.45 \pm 0.08) \text{ GeV}^{-1} \text{ m}^{-2} \text{ sr}^{-1} \text{ s}^{-1}$ and $\varphi_- = (1.11 \pm 0.01) \text{ GV}$ for the Pamela electron flux, and $C_- = (6.13 \pm 0.21) \text{ GeV}^{-1} \text{ m}^{-2} \text{ sr}^{-1} \text{ s}^{-1}$ for the Fermi-LAT electron flux. Though the data points published by these experiments are clearly inconsistent with the AMS data, the obtained fit parameters are within the uncertainties consistent with those given in Table 1, even without taking the uncertainty on the energy scales of PAMELA and Fermi-LAT into account.

Similar studies could be performed using the positron fraction and the combined $e^+ + e^-$ flux. However, a precise analysis is not possible from the published AMS results since these data sets are not statistically independent due to an overlap in the event samples.

4 Model independent constraints on the annihilation cross section

For this analysis, we assume that the cosmic ray fluxes consist of a smooth background component that originates at high energies from some unspecified astrophysical source and of a sub-dominant exotic contribution that originates from dark matter annihilation in the Galactic halo. The latter could account for additional structure on top of the background predictions. For the description of the shape of the astrophysical background, *i.e.* the null-hypothesis, we use Eqs. (2). We do not observe significant deviation from the assumed background in the measured fluxes. We then set constraints on leptophilic dark matter models using Wilks theorem [40], namely the upper limit value on the signal normalisation is obtained increasing its value until the χ^2 value differs by 2.71 from the null-hypotheses. The background model parameters are treated as nuisance parameters. We first compute 95% CL upper limits on the leading order $2 \rightarrow 2$ annihilation cross section. We set upper limits on the normalisation of a possible signal due to dark matter annihilation and we subsequently translate them into limits on the velocity averaged annihilation cross section. These limits and the median expected upper limits obtained from 1000 pseudo-data sets are shown in Fig. 3. The pseudo-data sets are generated according to the background model, namely assuming that no exotic dark matter contribution is present. For each of these data sets we repeat the calculation of the upper limits. The median upper limits are obtained taking for each mass the median value of the resulting distribution. Compared to [15] we find limits that are about a factor 2 weaker. Several aspects which contribute to this difference have been discussed already in the introduction. In addition, the different procedure to calculate the upper limits used in [15] leads in most cases to stronger limits.

We have investigated the impact of the energy scale uncertainty from the fit, of the choice of different cosmic ray propagation models and of the uncertainties on the antiproton production cross section. We find that including the uncertainties on the energy scale does not significantly affect the results for the upper limits. More relevant are the uncertainties due to the choice of the cosmic rays propagation scenario and dark matter halo model. To study the impact of the propagation models, we have computed the upper limit using the MIN, MED and MAX cosmic rays propagation parameters [27] for the NFW dark matter profile. We also re-computed the upper limits for a fixed propagation scenario (MED) and different dark matter profiles (Einasto [29, 41], Isothermal [42, 43], Burkert [44–47] and Moore [48]) and different dark matter normalisations at the location of the solar system ($\rho \in [0.25, 0.7] \text{ GeV}/\text{cm}^3$ [31]). The latter has the effect of trivially rescaling the upper limits curve and is the most relevant source of uncertainties. All astrophysical parameters have been taken from [27].

We have recomputed the upper limits including electroweak correction but no distinguishable features are noticeable. Indeed, multi-TeV dark matter masses can give rise to 10% corrections

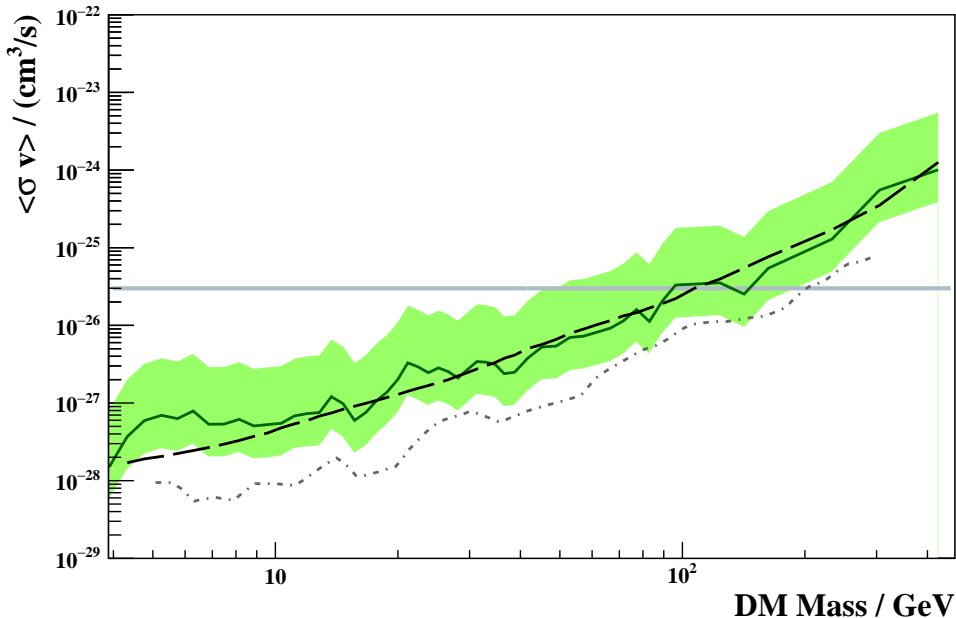


Figure 3: Solid line: 95% CL upper limits on the $2 \rightarrow 2$ annihilation cross section $\langle\sigma v\rangle$ for a generic model where dark matter annihilates at leading order only into electrons and positrons. The solid line is obtained for a specific choice of the dark matter distribution in the Galaxy (NFW profile) and for a specific choice of the propagation parameters (MED). Shaded band: estimate of the uncertainties due to different normalisations of the dark matter density at Earth, choice of the dark matter halo model and choice of the propagation model. Black dashed line: median expected upper limits. For comparison we show the results obtained in [15] (grey dashed-dotted line). Gray solid line: thermal relic cross section.

which are sizeable for collider studies but are negligible with respect to astrophysical uncertainties when computing dark matter upper limits.

5 Antiproton flux

A flux of antiprotons is generated by the radiation of electroweak gauge bosons, W^\pm and Z , off the primary standard model particles produced in the dark matter annihilation process. Thus, even for leptophilic dark matter models, antiprotons are produced and the antiproton flux can be compared to measurements to further test and constrain this model. For dark matter particles heavier than the electroweak gauge bosons, $M_{\text{DM}} \gg M_{W/Z}$, the contributions due to electroweak radiation can be calculated in a model independent way by using generalised fragmentation functions [19, 20]. The fragmentation function approach works for models where the leading-order annihilation cross section is not helicity suppressed, and it provides reliable results for masses $M_{\text{DM}} \gtrsim 5M_{W,Z} \approx 500 \text{ GeV}$ [19, 20]. However, as we are interested also in smaller dark matter masses, we consider the leptophilic dark matter model presented earlier as a representative model.

In the previous section we have derived model independent upper limits on the $2 \rightarrow 2$ cross section. The impact on the upper limits of including electroweak radiation is found to be negligible. However, the inclusion of electroweak radiation in our analysis is crucial as an antiproton flux is induced. Assuming that the dark matter annihilation cross section is at its upper limit value, *i.e.* the values represented by the black line in Fig. 3, we obtain predictions for the maximum antiproton-to-proton ratio due to dark matter annihilation. These predictions can be compared to the measurements done by the Pamela [49] and AMS-02 Collaboration [50],

as shown in Fig. 4 for representative masses. One of the most relevant source of uncertainty is the knowledge of the cross section for antiproton production. This has been extensively studied for instance in [51, 52], according to which the uncertainties can be roughly 50% outside the range where the antiproton productions cross section is measured.²

The choice of the cosmic ray propagation model is a second relevant source of uncertainty, dominant at low energies [52]. In Fig. 4 the background curve is the “fiducial” antiproton-to-proton astrophysical ratio presented in [53]. The uncertainties on the background are those derived in [53]. The predictions for the antiproton-to-proton ratio including a dark matter contribution shown in Fig. 4 are affected by the same uncertainties. For the sake of simplicity, we do not show them in the figure.

A more reliable estimate of the constraints on the dark matter model from the \bar{p}/p ratio would require a systematic study of the background uncertainties and the correlation with the dark matter signal as presented in *e.g.* ([54–56]). We defer such a more comprehensive analysis to a forthcoming publication.

Our analysis suggests that for dark matter masses near or above $\mathcal{O}(1 \text{ TeV})$ the antiproton flux receives a sizeable contribution due to dark matter annihilation in the Galaxy, even for leptophilic models. It is therefore possible to further constrain also leptophilic dark matter models using the complementary information contained in the antiproton flux measurements, in particular for very high dark matter masses $M_{\text{DM}} \gtrsim 1 \text{ TeV}$, as shown in Fig. 4. The antiproton flux thus becomes relevant only for large dark matter masses. This regime is where electroweak corrections become model independent due to the appearance of universal logarithms as shown in [19, 20]. However, to be able to obtain robust and quantitative conclusions a better understanding of the astrophysical phenomena relevant to charged cosmic ray propagation models is necessary, as well as improved measurements of the inclusive antiproton production cross section at colliders. Additional AMS measurements of cosmic rays fluxes and ratios, like the recent boron-to-carbon ratio [57], are expected to provide new input for the modelling of the propagation of charged cosmic rays in the Galaxy. Dedicated studies of antiproton production in proton to helium collisions performed by the LHCb collaboration [58, 59], could help to reduce the uncertainties on the antiproton production cross section.

6 Conclusions

We have proposed a simple phenomenological model which provides an excellent description of the electron and positron fluxes in cosmic rays as measured by AMS. Several important conclusions can be drawn from our results: *(i)* The minimal model from [17] cannot be used to derive values for the cutoff energy of its source term from a fit to the positron fraction alone because it is too simple and does not describe the individual fluxes. *(ii)* Neither the positron nor the electron flux shows any sharp spectral structures. At high energies, the positron flux is dominated by the source term while the electron flux is dominated by the diffuse term. *(iii)* The electron flux is consistent with a charge-symmetric source term. However, it can be shown that the electron flux alone can equally well be described by Eqs. (2) *without* a source term. To prove that the source term is indeed charge-symmetric as expected from dark matter models or astrophysical sources used to explain the observed positron excess, a solid description of the physical processes relevant for the diffuse term is needed. *(iv)* There is evidence for a spectral break in the electron flux at an energy of $\sim 30 \text{ GeV}$. This might be a useful reference point for the cross-calibration with future experiments. *(v)* The solar modulation parameters for positrons and electrons φ_+ and φ_- are significantly different. This shows that either the force-field approximation breaks down in the case of cosmic ray positrons and/or electrons or even

²For more details we refer to [51, 52] and references therein.

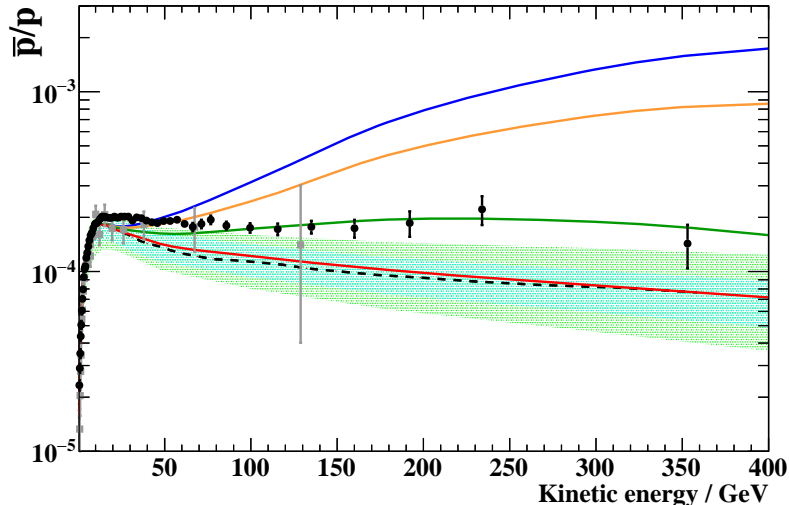


Figure 4: Black circles and grey squares: AMS-02 and PAMELA measurements, respectively. The solid lines represent the predictions for the antiproton-to-proton ratio for $M_{\text{DM}} = 425, 1000, 3000, 5000$ GeV (red, green, orange and blue, respectively). The antiproton flux consists of an astrophysical component, plus an exotic component due to dark matter annihilation in the Galaxy, normalised to the upper limit value of the leading order annihilation cross section. The estimate of the background (dashed black line) and its uncertainties are taken from [53]. More specifically, the blue band represent the uncertainties on the antiproton production cross section, while the green band represents those due to the choice of the propagation parameters. The dark matter signals are affected by the same sort of uncertainties, not drawn here for clarity.

more additional terms are needed in the model.

We would like to point out that the data points below 15 GeV are especially important to constrain the solar modulation parameters as well as the diffuse terms. Therefore, reliable statements about source parameters require a proper treatment of the time dependence of the cosmic ray electron and positron fluxes. At energies below 20 GeV, a time dependence of the fluxes can be expected, possibly exceeding the systematic uncertainties quoted on the average fluxes.

(vi) Even with our assumptions on the degree of correlation between the systematic uncertainties of the AMS data points, we find very good agreement of the data with a smooth model. On the other hand, it has been argued that a certain amount of spectral features (“bumpiness”) is expected in the fluxes of positrons and electrons if the standard paradigm for cosmic ray acceleration and propagation holds, namely from the contributions of individual sources, and that the absence of such features would constitute an anomaly in our understanding of cosmic rays [60].

We have used our improved phenomenological description of electron and positron fluxes to place limits on the dark matter annihilation cross section in leptophilic dark matter models. We find that (vii) an appropriate description of the background is crucial, especially for the low energy region, as most of the electrons and positrons produced via dark matter annihilation are soft, since they lose energy while propagating through the Galaxy. (viii) Within this class of models we exclude the region of the parameter space with $M_{\text{DM}} \lesssim 100$ GeV for a thermal relic, even though this bound is somewhat diluted by the uncertainty in the normalisation of the dark matter density. (ix) The inclusion of electroweak radiation has a very small impact on the upper limits on the dark matter annihilation cross section. However, contributions due to the radiation of electroweak gauge boson are of crucial importance as they induce correlation

among fluxes of different particles species and, in particular, predict an antiproton flux even within leptophilic dark matter models. This may allow to further constrain this class of models using measurements of the antiproton-to-proton ratio or antiproton flux. The comparison with Pamela and the recent AMS-02 data [50] suggests that we might be able to constrain the higher mass region ($M_{\text{DM}} \gtrsim 3 \text{ TeV}$) of the parameter space, even though a careful analysis of the uncertainties is needed in order to draw robust conclusions.

Acknowledgements

We acknowledge support by the German Research Foundation DFG through the research training group ‘‘Particle and Astroparticle Physics in the Light of the LHC’’, the Helmholtz Alliance for Astroparticle Physics (HAP) and the German Federal Ministry of Education and Research (BMBF).

References

- [1] **AMS** Collaboration, M. Aguilar *et al.*, *Electron and Positron Fluxes in Primary Cosmic Rays Measured with the Alpha Magnetic Spectrometer on the International Space Station*. [Phys.Rev.Lett. **113** \(2014\) 121102](#).
- [2] L. Feng, R.-Z. Yang, H.-N. He, T.-K. Dong, Y.-Z. Fan, and J. Chang, *AMS-02 positron excess: new bounds on dark matter models and hint for primary electron spectrum hardening*. [Phys. Lett. **B728** \(2014\) 250–255](#), [arXiv:1303.0530 \[astro-ph.HE\]](#).
- [3] I. Cholis and D. Hooper, *Dark Matter and Pulsar Origins of the Rising Cosmic Ray Positron Fraction in Light of New Data From AMS*. [Phys.Rev. **D88** \(2013\) 023013](#), [arXiv:1304.1840 \[astro-ph.HE\]](#).
- [4] M. Di Mauro, F. Donato, N. Fornengo, and A. Vittino, *Dark matter vs. astrophysics in the interpretation of AMS-02 electron and positron data*. [JCAP **1605** \(2016\) no. 05, 031](#), [arXiv:1507.07001 \[astro-ph.HE\]](#).
- [5] T. Linden and S. Profumo, *Probing the Pulsar Origin of the Anomalous Positron Fraction with AMS-02 and Atmospheric Cherenkov Telescopes*. [Astrophys. J. **772** \(2013\) 18](#), [arXiv:1304.1791 \[astro-ph.HE\]](#).
- [6] K. Kohri, K. Ioka, Y. Fujita, and R. Yamazaki, *Can we explain AMS-02 antiproton and positron excesses simultaneously by nearby supernovae without pulsars or dark matter?* [PTEP **2016** \(2016\) no. 2, 021E01](#), [arXiv:1505.01236 \[astro-ph.HE\]](#).
- [7] M. Boudaud *et al.*, *A new look at the cosmic ray positron fraction*. [Astron. Astrophys. **575** \(2015\) A67](#), [arXiv:1410.3799 \[astro-ph.HE\]](#).
- [8] M. Cirelli, M. Kadastik, M. Raidal, and A. Strumia, *Model-independent implications of the e^\pm , anti-proton cosmic ray spectra on properties of Dark Matter*. [Nucl.Phys. **B813** \(2009\) 1–21](#), [arXiv:0809.2409 \[hep-ph\]](#).
- [9] F. Donato, D. Maurin, P. Brun, T. Delahaye, and P. Salati, *Constraints on WIMP Dark Matter from the High Energy PAMELA \bar{p}/p data*. [Phys.Rev.Lett. **102** \(2009\) 071301](#), [arXiv:0810.5292 \[astro-ph\]](#).
- [10] L. Bergström, J. Edsjo, and G. Zaharijas, *Dark matter interpretation of recent electron and positron data*. [Phys.Rev.Lett. **103** \(2009\) 031103](#), [arXiv:0905.0333 \[astro-ph.HE\]](#).
- [11] D. P. Finkbeiner, L. Goodenough, T. R. Slatyer, M. Vogelsberger, and N. Weiner, *Consistent Scenarios for Cosmic-Ray Excesses from Sommerfeld-Enhanced Dark Matter Annihilation*. [JCAP **1105** \(2011\) 002](#), [arXiv:1011.3082 \[hep-ph\]](#).
- [12] Q. Yuan, X.-J. Bi, G.-M. Chen, Y.-Q. Guo, S.-J. Lin, *et al.*, *Implications of the AMS-02*

- positron fraction in cosmic rays.* *Astropart.Phys.* **60** (2015) 1–12, [arXiv:1304.1482 \[astro-ph.HE\]](#).
- [13] H.-B. Jin, Y.-L. Wu, and Y.-F. Zhou, *Implications of the first AMS-02 measurement for dark matter annihilation and decay.* *JCAP* **1311** (2013) 026, [arXiv:1304.1997 \[hep-ph\]](#).
- [14] G. Bertone, M. Cirelli, A. Strumia, and M. Taoso, *Gamma-ray and radio tests of the $e+e-$ excess from DM annihilations.* *JCAP* **0903** (2009) 009, [arXiv:0811.3744 \[astro-ph\]](#).
- [15] L. Bergström, T. Bringmann, I. Cholis, D. Hooper, and C. Weniger, *New limits on dark matter annihilation from Alpha Magnetic Spectrometer Cosmic Ray Positron Data.* *Phys.Rev.Lett.* **111** (2013) 171101, [arXiv:1306.3983 \[astro-ph.HE\]](#).
- [16] A. Ibarra, A. S. Lamperstorfer, and J. Silk, *Dark matter annihilations and decays after the AMS-02 positron measurements.* *Phys. Rev.* **D89** (2014) no. 6, 063539, [arXiv:1309.2570 \[hep-ph\]](#).
- [17] **AMS** Collaboration, M. Aguilar *et al.*, *First Result from the Alpha Magnetic Spectrometer on the International Space Station: Precision Measurement of the Positron Fraction in Primary Cosmic Rays of 0.5 – 350 GeV.* *Phys.Rev.Lett.* **110** (2013) 141102.
- [18] S. Schael, *New results from the AMS experiment on the International Space Station*, TeV Particle Astrophysics, CERN, 15 Sep 2016.
- [19] P. Ciafaloni, D. Comelli, A. Riotto, F. Sala, A. Strumia, *et al.*, *Weak Corrections are Relevant for Dark Matter Indirect Detection.* *JCAP* **1103** (2011) 019, [arXiv:1009.0224 \[hep-ph\]](#).
- [20] L. Ali Cavazonza, M. Krämer, and M. Pellen, *Electroweak fragmentation functions for dark matter annihilation.* *JCAP* **1502** (2015) no. 02, 021, [arXiv:1409.8226 \[hep-ph\]](#).
- [21] G. Servant and T. M. Tait, *Is the lightest Kaluza-Klein particle a viable dark matter candidate?* *Nucl.Phys.* **B650** (2003) 391–419, [arXiv:hep-ph/0206071 \[hep-ph\]](#).
- [22] K. Kong and K. T. Matchev, *Precise calculation of the relic density of Kaluza-Klein dark matter in universal extra dimensions.* *JHEP* **0601** (2006) 038, [arXiv:hep-ph/0509119 \[hep-ph\]](#).
- [23] A. Belyaev, N. D. Christensen, and A. Pukhov, *CalcHEP 3.4 for collider physics within and beyond the Standard Model.* *Comput.Phys.Commun.* **184** (2013) 1729–1769, [arXiv:1207.6082 \[hep-ph\]](#).
- [24] A. Datta, K. Kong, and K. T. Matchev, *Minimal Universal Extra Dimensions in CalcHEP/CompHEP.* *New J.Phys.* **12** (2010) 075017, [arXiv:1002.4624 \[hep-ph\]](#).
- [25] J. Alwall, R. Frederix, S. Frixione, V. Hirschi, F. Maltoni, *et al.*, *The automated computation of tree-level and next-to-leading order differential cross sections, and their matching to parton shower simulations.* *JHEP* **1407** (2014) 079, [arXiv:1405.0301 \[hep-ph\]](#).
- [26] T. Sjostrand, S. Mrenna, and P. Z. Skands, *A Brief Introduction to PYTHIA 8.1.* *Comput.Phys.Commun.* **178** (2008) 852–867, [arXiv:0710.3820 \[hep-ph\]](#).
- [27] M. Cirelli, G. Corcella, A. Hektor, G. Hutsi, M. Kadastik, *et al.*, *PPPC 4 DM ID: A Poor Particle Physicist Cookbook for Dark Matter Indirect Detection.* *JCAP* **1103** (2011) 051, [arXiv:1012.4515 \[hep-ph\]](#).
- [28] J. F. Navarro, C. S. Frenk, and S. D. White, *The Structure of cold dark matter halos.* *Astrophys.J.* **462** (1996) 563–575, [arXiv:astro-ph/9508025 \[astro-ph\]](#).
- [29] J. F. Navarro, A. Ludlow, V. Springel, J. Wang, M. Vogelsberger, *et al.*, *The Diversity and Similarity of Cold Dark Matter Halos.* [arXiv:0810.1522 \[astro-ph\]](#).
- [30] F. Donato, N. Fornengo, D. Maurin, and P. Salati, *Antiprotons in cosmic rays from neutralino annihilation.* *Phys. Rev.* **D69** (2004) 063501, [arXiv:astro-ph/0306207 \[astro-ph\]](#).
- [31] J. Bovy and S. Tremaine, *On the local dark matter density.* *Astrophys.J.* **756** (2012) 89, [arXiv:1205.4033 \[astro-ph.GA\]](#).

- [32] M. Di Mauro, F. Donato, N. Fornengo, R. Lineros, and A. Vittino, *Interpretation of AMS-02 electrons and positrons data*. *JCAP* **1404** (2014) 006, [arXiv:1402.0321 \[astro-ph.HE\]](#).
- [33] L. Gleeson and W. Axford, *Solar Modulation of Galactic Cosmic Rays*. *Astrophys.J.* **154** (1968) 1011.
- [34] **AMS** Collaboration, M. Aguilar *et al.*, *Precision Measurement of the ($e^+ + e^-$) Flux in Primary Cosmic Rays from 0.5 GeV to 1 TeV with the Alpha Magnetic Spectrometer on the International Space Station*. *Phys.Rev.Lett.* **113** (2014) 221102.
- [35] **AMS** Collaboration, M. Aguilar *et al.*, *Precision Measurement of the Proton Flux in Primary Cosmic Rays from Rigidity 1 GV to 1.8 TV with the Alpha Magnetic Spectrometer on the International Space Station*. *Phys.Rev.Lett.* **114** (2015) no. 17, 171103.
- [36] J. Heinrich and L. Lyons, *Systematic errors*. *Ann. Rev. Nucl. Part. Sci.* **57** (2007) 145–169.
- [37] **PAMELA** Collaboration, O. Adriani *et al.*, *Cosmic-Ray Positron Energy Spectrum Measured by PAMELA*. *Phys. Rev. Lett.* **111** (2013) 081102, [arXiv:1308.0133 \[astro-ph.HE\]](#).
- [38] **PAMELA** Collaboration, O. Adriani *et al.*, *The cosmic-ray electron flux measured by the PAMELA experiment between 1 and 625 GeV*. *Phys. Rev. Lett.* **106** (2011) 201101, [arXiv:1103.2880 \[astro-ph.HE\]](#).
- [39] **Fermi-LAT** Collaboration, M. Ackermann *et al.*, *Measurement of separate cosmic-ray electron and positron spectra with the Fermi Large Area Telescope*. *Phys. Rev. Lett.* **108** (2012) 011103, [arXiv:1109.0521 \[astro-ph.HE\]](#).
- [40] S. S. Wilks, *The Large-Sample Distribution of the Likelihood Ratio for Testing Composite Hypotheses*. *Annals Math. Statist.* **9** (1938) no. 1, 60–62.
- [41] A. W. Graham, D. Merritt, B. Moore, J. Diemand, and B. Terzic, *Empirical models for Dark Matter Halos. I. Nonparametric Construction of Density Profiles and Comparison with Parametric Models*. *Astron.J.* **132** (2006) 2685–2700, [arXiv:astro-ph/0509417 \[astro-ph\]](#).
- [42] K. Begeman, A. Broeils, and R. Sanders, *Extended rotation curves of spiral galaxies: Dark haloes and modified dynamics*. *Mon.Not.Roy.Astron.Soc.* **249** (1991) 523.
- [43] J. N. Bahcall and R. Soneira, *The Universe at faint magnetitudes. 2. Models for the predicted star counts*. *Astrophys.J.Suppl.* **44** (1980) 73–110.
- [44] A. Burkert, *The Structure of dark matter halos in dwarf galaxies*. *IAU Symp.* **171** (1996) 175, [arXiv:astro-ph/9504041 \[astro-ph\]](#).
- [45] P. Salucci and A. Burkert, *Dark matter scaling relations*. *Astrophys.J.* **537** (2000) L9–L12, [arXiv:astro-ph/0004397 \[astro-ph\]](#).
- [46] G. Gentile, P. Salucci, U. Klein, D. Vergani, and P. Kalberla, *The Cored distribution of dark matter in spiral galaxies*. *Mon.Not.Roy.Astron.Soc.* **351** (2004) 903, [arXiv:astro-ph/0403154 \[astro-ph\]](#).
- [47] P. Salucci, A. Lapi, C. Tonini, G. Gentile, I. Yegorova, *et al.*, *The Universal Rotation Curve of Spiral Galaxies. 2. The Dark Matter Distribution out to the Virial Radius*. *Mon.Not.Roy.Astron.Soc.* **378** (2007) 41–47, [arXiv:astro-ph/0703115 \[ASTRO-PH\]](#).
- [48] J. Diemand, B. Moore, and J. Stadel, *Convergence and scatter of cluster density profiles*. *Mon.Not.Roy.Astron.Soc.* **353** (2004) 624, [arXiv:astro-ph/0402267 \[astro-ph\]](#).
- [49] **PAMELA** Collaboration, O. Adriani *et al.*, *PAMELA results on the cosmic-ray antiproton flux from 60 MeV to 180 GeV in kinetic energy*. *Phys.Rev.Lett.* **105** (2010) 121101, [arXiv:1007.0821 \[astro-ph.HE\]](#).
- [50] **AMS** Collaboration, M. Aguilar *et al.*, *Antiproton Flux, Antiproton-to-Proton Flux Ratio, and Properties of Elementary Particle Fluxes in Primary Cosmic Rays Measured with the Alpha Magnetic Spectrometer on the International Space Station*. *Phys. Rev. Lett.* **117**

- (2016) no. 9, .
- [51] F. Donato, D. Maurin, P. Salati, A. Barrau, G. Boudoul, and R. Taillet, *Anti-protons from spallations of cosmic rays on interstellar matter*. *Astrophys. J.* **563** (2001) 172–184, [arXiv:astro-ph/0103150](#) [[astro-ph](#)].
 - [52] M. di Mauro, F. Donato, A. Goudelis, and P. D. Serpico, *New evaluation of the antiproton production cross section for cosmic ray studies*. *Phys. Rev.* **D90** (2014) no. 8, 085017, [arXiv:1408.0288](#) [[hep-ph](#)].
 - [53] G. Giesen, M. Boudaud, Y. Gnolini, V. Poulin, M. Cirelli, P. Salati, and P. D. Serpico, *AMS-02 antiprotons, at last! Secondary astrophysical component and immediate implications for Dark Matter*. *JCAP* **1509** (2015) no. 09, 023, [arXiv:1504.04276](#) [[astro-ph.HE](#)].
 - [54] M. Korsmeier and A. Cuoco, *Galactic cosmic-ray propagation in the light of AMS-02: Analysis of protons, helium, and antiprotons*. *Phys. Rev.* **D94** (2016) no. 12, 123019, [arXiv:1607.06093](#) [[astro-ph.HE](#)].
 - [55] A. Cuoco, M. Krämer, and M. Korsmeier, *Novel dark matter constraints from antiprotons in the light of AMS-02*. [arXiv:1610.03071](#) [[astro-ph.HE](#)].
 - [56] M.-Y. Cui, Q. Yuan, Y.-L. S. Tsai, and Y.-Z. Fan, *A possible dark matter annihilation signal in the AMS-02 antiproton data*. [arXiv:1610.03840](#) [[astro-ph.HE](#)].
 - [57] **AMS** Collaboration, M. Aguilar *et al.*, *Precision Measurement of the Boron to Carbon Flux Ratio in Cosmic Rays from 1.9 GV to 2.6 TV with the Alpha Magnetic Spectrometer on the International Space Station*. *Phys. Rev. Lett.* **117** (2016) no. 23, 231102.
 - [58] L. Massacrier, CERN Seminar, 28 June 2016.
 - [59] *SMOG as a Fixed target in the LHC*, <https://lbtwiki.cern.ch/bin/view/velo/smogasfixedtarget>.
 - [60] P. Serpico, *Possible physics scenarios behind cosmic-ray anomalies*. 34th International Cosmic Ray Conference (ICRC), The Hague, The Netherlands (2015) .